Journal of Computational Electronics 2: 487–490, 2003

Effect of Shape and Size on Electron Transition Energies for Nanoscale InAs/GaAs Quantum Rings

YIMING LI*
Department of Nano Device Technology, National Nano Device Laboratories, Hsinchu 300, Taiwan; Microelectronics and Information Systems Research Center, National Chiao Tung University, Hsinchu 300, Taiwan
ymli@mail.nctu.edu.tw

HSIAO-MEI LU
Department of Bioengineering, University of Illinois at Chicago, Chicago, Illinois 60612, USA

Abstract. In this paper, we study the impact of the sizes and the shapes of nanoscale semiconductor quantum rings on the electron and hole energy states. A three-dimensional effective one band Schrödinger equation is solved numerically for semiconductor quantum rings with disk, cut-bottom-elliptical, and conical shapes. For small InAs/GaAs quantum rings we have found a sufficient difference in the ground state and excited state ($l = -1$) electron energies for rings with the same volume but different shapes. Volume dependence of the electron and hole energies can vary over a wide range and depends significantly on the ring shapes. It is found that a non-periodical oscillation of the energy band gap between the lowest electron and hole states as a function of external magnetic fields.

Keywords: nanoscale quantum ring, InAs/GaAs, energy spectra, geometry and magnetic field effects, computer simulation

1. Introduction

Advances in the fabrication of semiconductor nanostructures have generated a huge quantity of experimental and theoretical data in this topic [1–13]. The three-dimensional (3D) confinement of charge carriers in those structures allows very rich optical and magnetic characteristics which potentially may have very important device applications [1–6]. The study of semiconductor nanoscale quantum rings significantly connects the gap between quantum dots and meso-scopic quantum ring structures. The spectral variation in semiconductor quantum rings caused by the non-uniformity in the size and shape is important for magneto-optical properties and practical device applications. Various experimental results suggest that InAs/GaAs quantum rings can have disk (DI), cut-bottom-elliptical (EL), or conical (CO) shapes with a circular top view cross section and a large area-to-height aspect ratio [7–10]. To the best of our knowledge, analysis of the influence of the ring size and shape on the electron energy states has not been done yet.

In this study, we calculate and compare the electron energy spectra for 3D nanoscale InAs/GaAs quantum rings of three different shapes (see Fig. 1): DI, EL, and CO shapes. Our model considers: (1) the position dependent effective mass Hamiltonian in non-parabolic approximation for electrons; (2) the position dependent effective mass Hamiltonian in parabolic approximation for holes; (3) the finite hard wall confinement potential; and (4) the Ben Daniel-Duke boundary conditions. To solve this 3D nonlinear problem, the nonlinear iterative method [11–13] is improved to calculate "self-consistent" solutions more efficiently. It is found that

*To whom correspondence should be addressed.

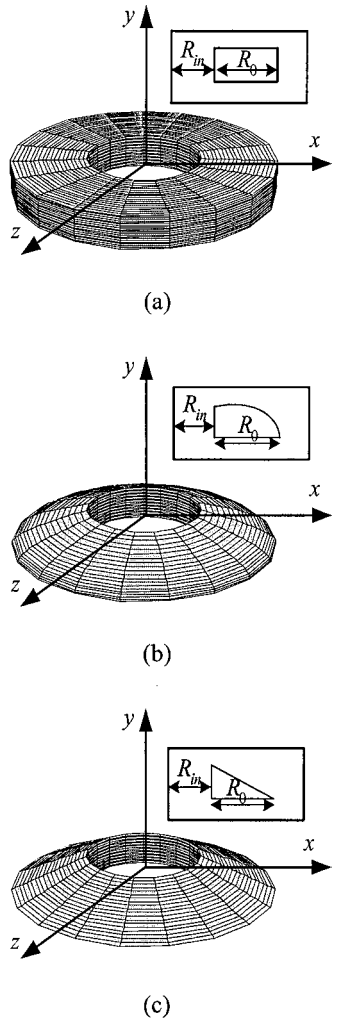

Figure 1. Quantum rings with different shapes: (a) DI, (b) EL and (c) CO.

the volume dependence of electron and hole energies can vary over a wide range and depends on the ring shapes. The variations of the ring size and shape produce an energy change up to an order of 0.15 eV in the strong confinement region. The energy band gap versus the magnetic field depends on the ring volume and transits non-periodically.

This paper is organized as follows. Section 2 is the modeling and simulation. Section 3 describes results of calculations. Section 4 draws the conclusion.

2. Theoretical Model and Computational Method

We consider the DI-, EL-, and CO-shaped quantum rings with the hard-wall confinement potential [12,13]. The effective mass Hamiltonian for electrons ($c = e$) and holes ($c = h$) is

$$\hat{H}_c = \Pi_{\mathbf{r}} \frac{1}{2m_c(E, \mathbf{r})} \Pi_{\mathbf{r}} + V_c(\mathbf{r}) + \frac{1}{2} g_c(E, \mathbf{r}) \mu_B \mathbf{B}\boldsymbol{\sigma}, \tag{1}$$

where $\Pi_{\mathbf{r}} = -i\hbar\nabla_{\mathbf{r}} + e\mathbf{A}(\boldsymbol{r})$ represents the electron momentum vector. $\nabla_{\mathbf{r}}$ is the spatial gradient, $\mathbf{A}(\boldsymbol{r})$ is the vector potential, and $\mathbf{B} = curl\mathbf{A}$ is the magnetic field. For electrons, the electron effective mass follows

$$\frac{1}{m_e(E, \mathbf{r})} = \frac{2P^2}{3\hbar^2}\left[\frac{2}{E + E_g(\mathbf{r}) - V_e(\mathbf{r})} + \frac{1}{E + E_g(\mathbf{r}) - V_e(\mathbf{r}) + \Delta(\mathbf{r})}\right], \tag{2}$$

and Landé factor is

$$g_e(E, \mathbf{r}) = 2\left\{1 - \frac{m_0}{m_e(E, \mathbf{r})} \frac{\Delta(\mathbf{r})}{3(E + E_g(\mathbf{r})) + 2\Delta(\mathbf{r})}\right\}. \tag{3}$$

$V_e(\boldsymbol{r})$ is the confinement potential, $E_g(\boldsymbol{r})$ and $\Delta(\boldsymbol{r})$ are the position-dependent band gap and spin-orbit splitting in the valence band, P is the momentum matrix element, $\boldsymbol{\sigma}$ is the vector of the Pauli matrixes, and m_0 and e are the free-electron elementary mass and charge, respectively. For holes, $m_h(E, \boldsymbol{r})$ and $g_h(E, \boldsymbol{r})$ are assumed to be only position dependent. We consider the hard-wall confinement potential $V_c(\mathbf{r}) = 0$ for $\mathbf{r}$ inside the ring (I) and $V_c(\mathbf{r}) = V_{c0}$ for $\mathbf{r}$ outside the ring (II), where V_{c0} is the band offset. The Ben Daniel-Duke boundary conditions for the electron and hole wave functions $\Psi(\mathbf{r})$ are $\Psi_{cI}(\mathbf{r}_s) = \Psi_{cII}(\mathbf{r}_s)$ and $(\hbar^2/2m_c(E, \mathbf{r}))\nabla_{\mathbf{r}}|_n \Psi_i(\mathbf{r}_s) = \text{constant}$, where $\mathbf{r}_s$ is the position of the system interface. All rings are cylindrically symmetric with respect to the base radius and height in the coordinates (R, ϕ, z), so the wave function can be written as $\Psi_c(\mathbf{r}) = \Phi_c(R, z)\exp(il\phi)$, where $l = 0, \pm1, \pm2, \ldots$ is the orbital quantum number, and the problem is in the coordinate (R, z). The Schrödinger equation for electrons and holes is

$$\begin{aligned} &-\frac{\hbar^2}{2m_{ci}(E)}\left(\frac{\partial^2}{\partial R^2} + \frac{\partial}{R\partial R} + \frac{\partial^2}{\partial z^2} - \frac{l^2}{R^2}\right)\Phi_{ci}(R, z) \\ &+\left(\frac{m_{ci}(E)\Omega_{ci}^2(E)R^2}{8} + s\frac{\mu_B}{2}g_{ci}(E)\mathbf{B}\right. \\ &\left.+\frac{\hbar\Omega_{ci}(E)}{2}l + V_{c0}\delta_{iII}\right)\Phi_{ci}(R, z) \\ &= E\Phi_{ci}(R, z), \end{aligned} \tag{4}$$

where $i = I, II$, $\Omega_{ci}(E) = e\mathbf{B}/m_{ci}(E)$, and $s = \pm 1$ is the orientation of the electron spin along the z-axis. The boundary conditions are $\Phi_{cI}(R, z) = \Phi_{cII}(R, z)$, and

$$\frac{1}{m_{cI}(E)}\left\{\frac{\partial\Phi_{cI}(R,z)}{\partial R} + \frac{df(R)}{dR}\frac{\partial\Phi_{cI}(R,z)}{\partial z}\right\}\Bigg|_{z=f(R)} = \frac{1}{m_{cII}(E)}\left\{\frac{\partial\Phi_{cII}(R,z)}{\partial R} + \frac{df(R)}{dR}\frac{\partial\Phi_{cII}(R,z)}{\partial z}\right\}\Bigg|_{z=f(R)}, \quad (5)$$

where $z = f(R)$ on the $\{R, z\}$ plane is a contour generator for all ring structures.

The energy band gap $E_g(\mathbf{B}) = E_{ge}(\mathbf{B}) + E_{gh}(\mathbf{B}) + E_{gR}$, where E_{ge} and E_{gh} are the ground state energies for electrons and holes, and E_{gR} is the energy gap in the quantum ring. The energy dependence of the electron effective mass and Landé factor complicates the analytical solution considerably. Computer simulation of energy spectra for quantum rings is suggested. For each applied magnetic field, the effective mass and Landé factor are calculated with an arbitrary initial energy $E = E_0$. The finite volume [14] discretized Schrödinger equation is solved to calculate all bounded energy levels. To solve the corresponding matrix eigenvalue problem more efficiently, a hybrid computational scheme is suggested. This scheme combines the robust balanced and shifted QR method [15] with the fast implicitly restarted Arnoldi [16]. If E converges, we calculate $E_g(\mathbf{B})$; else we update the newer E and perform the next iteration. The generalized method for solving different shape quantum rings converges monotonically and is cost effective

3. Results and Discussion

In Fig. 2 we present the calculated electron energy levels for InAs/GaAs quantum rings as functions of the ring volume. For InAs, E_{1g} is 0.42 eV, Δ_1 is 0.38 eV, and $m_{1e}(0) = 0.024m_0$. For GaAs, E_{2g} is 1.52 eV, $\Delta_2 = 0.34$ eV, $m_{2e}(0) = 0.067m_0$, and $V_0 = 0.77$ eV. From experimental data [6–9], the base radius of the rings $R_0 = 20$ nm and the inner radius $R_{\text{in}} = 10$ nm for all shapes. Our model predicts electron energy dependences on the volume for rings of different shapes. When the ring volume increases, the energy states of different shapes converge. The most sensitive to the ring volume variation is the DI shape and, the least one is the CO shape rings. This is no surprise since the electron wave function is the best confined for the disk geometry when the volume and the radius are fixed. The wave function shape confirms weaker confinement for CO-shaped rings. The excited state ($l = -1$), however, has demonstrated a weaker sensitivity to the ring shape and volume (see the right one of Fig. 2). This is because that the electron wave functions of the exited states are less confined and, therefore, are less sensitive to the ring shape and size.

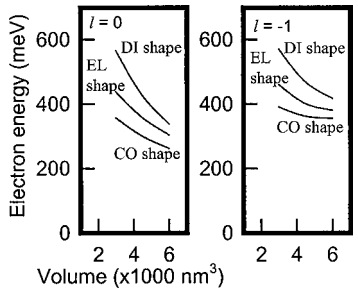

Figure 2. The electron ground state (the left figure) and the $l = -1$ excited state (the right one) energies versus the ring volume at $\mathbf{B} = 0$ T.

Using the same calculation method, we obtained hole energy states for rings of the same shapes. The hole effective mass is taken as $m_{1h} = 0.4m_0$ and $m_{2h} = 0.5m_0$, and band offset $V_0 = 0.33$ eV. Shown in Fig. 3 is the hole energy states for the ground (the left figure) and $l = -1$ excited (the right one) states. With this same parameter setting Fig. 4 shows the electron and hole energy versus $\mathbf{B}$ for the DI-shaped quantum ring, where the ring volume 3000 nm^3 is fixed. The energy states are numerated by a set of quantum numbers $\{n, l, s\}$, where $n = 0, 1, 2, \ldots$ is the main quantum

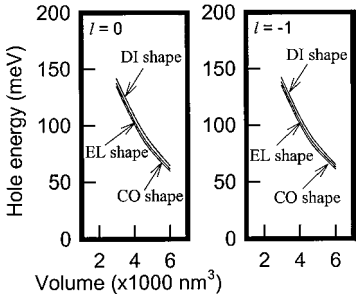

Figure 3. The hole ground state (the left figure) and the $l = -1$ excited state (the right one) energies versus the ring volume at $\mathbf{B} = 0$ T.

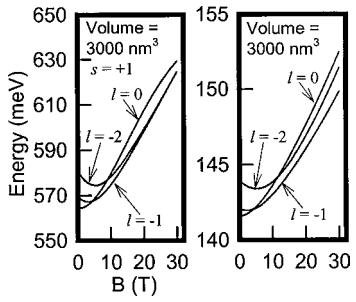

Figure 4. Plots of electron (the left figure) and hole (the right one) energies versus **B** for the DI-shaped quantum ring with volume = 3000 nm^3.

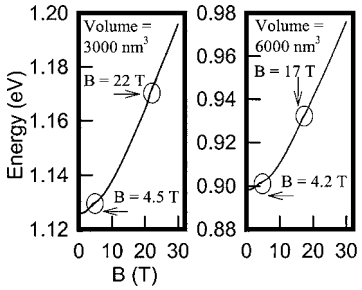

Figure 5. The energy band gap versus **B** for the DI-shaped quantum ring with volume = 3000 nm^3 (the left figure) and 6000 nm^3 (the right one).

number. The left figure of Fig. 4 is the electron energy $E_{0,l,+1}$ for $l = 0, -1$, and -2. The calculated results of the energy band gap between the lowest electron and hole states for the InAs/GaAs quantum ring with volumes 3000 and 6000 nm^3 are shown in Fig. 5. We find a non-periodical oscillation of $E_g(\mathbf{B})$ between the lowest electron and hole states as a function of **B**. The transition of $E_g(\mathbf{B})$ depends on the ring volume. Due to the wave function penetration into the torus region, it is found $E_g(\mathbf{B})$ does not follow the 1D periodical rule: $\pi(R_{\text{in}} + R)^2\mathbf{B}/\Theta_0 = n$, where n is an integer number and Θ_0 is the quantum of magnetic flux [13]. $E_g(\mathbf{B})$ depends on ring volume, and its non-periodical oscillation directs to our 3D modeling and simulation. The results should be examined in the magnetic-photo-luminescence spectra for nanoscale quantum rings.

4. Conclusions

We have presented a computational approach that allows us to study the electron and hole energy states for nanoscale semiconductor quantum rings of three different shapes. This method is useful to analyze the dependence of the quantum ring spectra on the ring volume and shape distributions. We found a large difference for the electron ground state energy in InAs/GaAs rings of the same volume but different shapes. The energy states of holes and transition energies under external magnetic fields were estimated. Our results advised that the non-periodical oscillation of energy band gap depends on the ring volume.

Acknowledgment

This work is supported in part by the National Science Council of TAIWAN under under contract numbers NSC-92-2112-M-429-001 and NSC-92-2815-C-492-001-E. It is also supported in part by the grant of the Ministry of Economic Affairs, Taiwan under contract No. 91-EC-17-A-07-S1-0011.

References

1. S. Parkin, J. Xin, C. Kaiser *et al.*, *Proceedings of the IEEE*, **91**, 661 (2003).
2. M. Bayer, M. Korkusinski, P. Hawrylak *et al. Phys. Rev. Lett.*, **90**, 186801 (2003).
3. F. Pederiva, A. Emperador, and E. Lipparini, *Phys. Rev.*, **B66**, 165314 (2002).
4. A. Fuhrer, S. Luscher, T. Ihn *et al.*, *Nature*, **413**, 822 (2001).
5. D. Bimberg, M. Grundmann, F. Heinrichsdorff *et al.*, *Thin Solid Films*, **367**, 235 (2000).
6. A.G. Aronov and Yu. V. Sharvin, *Rev. Mod. Phys.*, **59**, 755 (1987).
7. R. Blossey and A. Lorke, *Phys. Rev.*, **E65**, 021603 (2002).
8. J. Planelles, W. Jaskólski, and J.I. Aliaga, *Phys. Rev.*, **B65**, 033306 (2002).
9. A. Lorke, R.J. Luyken, A.O. Govorov *et al.*, *Phys. Rev. Lett.*, **84**, 2223 (2000).
10. A. Bruno-Alfonso and A. Latgé, *Phys. Rev.*, **B61**, 15887 (2000).
11. Y. Li *et al.*, *Comput. Phys. Commun.*, **141**, 66 (2001).
12. Y. Li *et al.*, *J. Comput. Elec.*, **1**, 227 (2002).
13. Y. Li and H.-M. Lu, *Jpn. J Appl. Phys.*, **42**, 2404 (2003).
14. R.S. Varga, *Matrix Iterative Analysis* (Springer, Berlin, 2000).
15. D. Watkins, *J. Comput. Appl. Math.*, **123**, 67 (2000).
16. D.C. Sorensen, *SIAM J. Matrix Anal. Appl.*, **13**, 357 (1992).